JACS
JOURNAL OF THE AMERICAN CHEMICAL SOCIETY
Article
pubs.acs.org/JACS

# A Facile Solution-Phase Approach to Transparent and Conducting ITO Nanocrystal Assemblies

Jonghun Lee,[†] Sunghwan Lee,[‡] Guanglai Li,[§] Melissa A. Petruska,[∥] David C. Paine,[‡] and Shouheng Sun*[,†,§]

[†]Department of Chemistry, [‡]School of Engineering, and [§]Institute of Molecular and Nanoscale Innovation, Brown University, Providence, Rhode Island 02912, United States

[∥]Advanced Technology Materials, Inc. (ATMI), Danbury, Connecticut 06810, United States

Supporting Information

**ABSTRACT:** Monodisperse 11 nm indium tin oxide (ITO) nanocrystals (NCs) were synthesized by thermal decomposition of indium acetylacetonate, $In(acac)_3$, and tin bis(acetylacetonate)dichloride, $Sn(acac)_2Cl_2$, at 270 °C in 1-octadecene with oleylamine and oleic acid as surfactants. Dispersed in hexane, these ITO NCs were spin-cast on centimeter-wide glass substrates, forming uniform ITO NC assemblies with root-mean-square roughness of 2.9 nm. The assembly thickness was controlled by ITO NC concentrations in hexane and rotation speeds of the spin coater. Via controlled thermal annealing at 300 °C for 6 h under Ar and 5% $H_2$, the ITO NC assemblies became conductive and transparent with the 146 nm-thick assembly showing $5.2 \times 10^{-3}$ Ω·cm ($R_s$ = 356 Ω/sq) resistivity and 93% transparency in the visible spectral range—the best values ever reported for ITO NC assemblies prepared from solution phase processes. The stable hexane dispersion of ITO NCs was also readily spin-cast on polyimide ($T_g$ ~360 °C), and the resultant ITO assembly exhibited a comparable conductivity and transparency to the assembly on a glass substrate. The reported synthesis and assembly provide a promising solution to the fabrication of transparent and conducting ITO NCs on flexible substrates for optoelectronic applications.

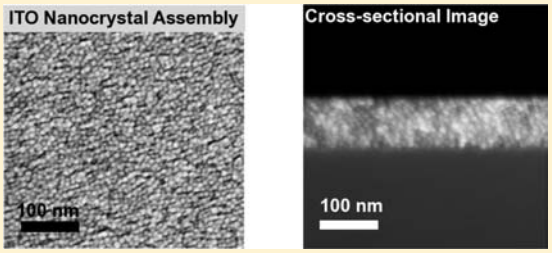


## INTRODUCTION

Indium tin oxides (ITOs) represent a group of well-known oxide materials that are both optically transparent and electrically conductive for use as transparent electrodes in organic light emitting diodes[1] and solar cells.[2] ITO has the basic crystal structure of indium oxide, $In_2O_3$, with $Sn^{4+}$ having an aliovalent substitution of $In^{3+}$. Its transparency to visible light comes from its large band gap energy between 3.5 and 4.3 eV,[1] while its conductivity originates from its intrinsic oxygen vacancies and/or extrinsic defects caused by $Sn^{4+}$ doping.[3] Transparent and conducting ITOs for optoelectronic applications are prepared in thin film forms by sputtering and have resistivities down to the $10^{-4}$ Ω·cm level and transparency greater than 85% in the visible spectral range.[1,4] However, sputtering cannot be readily used to control the patterns of ITO films on flexible substrates[5] and has a production yield generally lower than 30%.[6,7]

Compared to sputtering, the synthesis and deposition of ITO nanocrystals (NCs) from solution phase should be an attractive and promising alternative for ITO film fabrication and patterning:[8] the synthesis from solution leads to the formation of ITO NCs with controlled size, morphology and composition; and well-dispersed ITO NCs can also serve as inks for inkjet printing and roll-to-roll production.[8,9] Recent advances in solution phase syntheses have demonstrated that monodisperse NCs can be synthesized and assembled into uniform NC assemblies via cost-effective self-assembly methods.[10−13] However, similar synthesis and self-assembly approaches have not been successful in fabricating ITO assemblies with desired properties. ITO NCs are usually prepared via high-temperature reactions in an organic solution phase,[14−17] solvothermal reactions in an autoclave,[18,19] microwave-assisted reactions,[9] or sol−gel reactions on substrates.[20] Because of the limited size and morphology control, these ITO NCs are difficult to deposit into thin film forms. Instead, they are typically compressed into micrometer thick pellets and/or sintered at temperatures greater than 400 °C. As a result, they are nontransparent and highly resistive (with resistivities higher than $3 \times 10^{-2}$ Ω·cm), and are unsuitable for optoelectronic applications.

Here, we report a facile solution-phase synthesis of monodisperse ITO NCs and a spin-casting method to assemble these NCs on centimeter-wide glass substrates to form densely packed ITO NC arrays with high conductivity and transparency. Different from previous methods, our synthesis yielded monodisperse (standard deviation in diameter at 5%) 11 nm ITO NCs with composition tunable from 0 to 12 Sn atom %. More importantly, using spin-casting, we deposited ITO NCs uniformly on a glass substrate and controlled

Received: May 17, 2012
Published: July 21, 2012

   dx.doi.org/10.1021/ja3044807 | J. Am. Chem. Soc. 2012, 134, 13410−13414

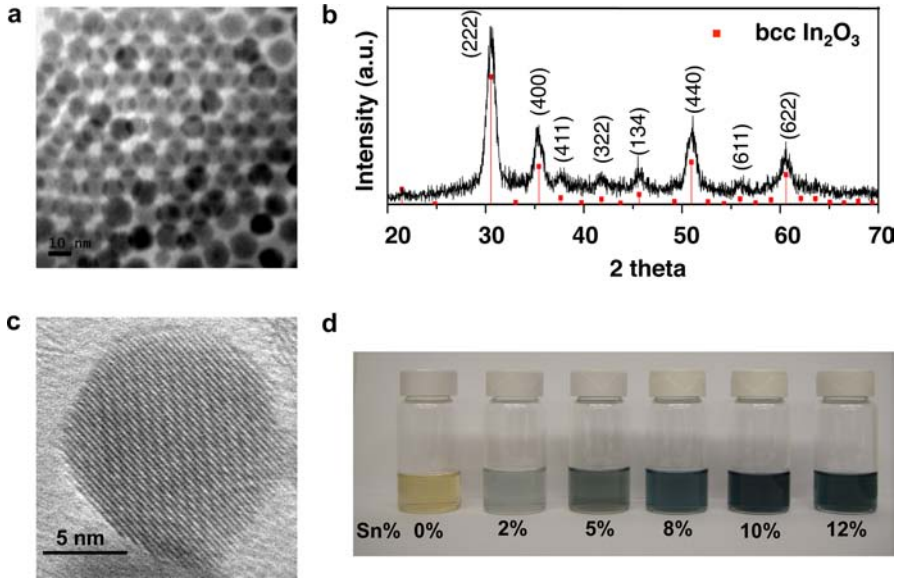


**Figure 1.** ITO NCs synthesized via a solution-phase reaction. (a) TEM image of self-assembled ITO NCs; (b) XRD of ITO NCs; (c) HRTEM image of a single ITO NC; (d) photograph of a series of ITO NC dispersions in hexane with different Sn compositions.

assembly thickness from 30 to 146 nm. Treated under a controlled thermal annealing condition, these assemblies showed thickness-dependent resistivity and transparency. The 146 nm thick ITO NC assembly annealed under Ar and 5% $H_2$ at 300 °C exhibited a resistivity of $5.2 \times 10^{-3}$ Ω·cm and transparency as high as 93%—these are the best values ever reported for an ITO NC assembly obtained from a solution-phase process. Furthermore, the stable hexane dispersion of ITO NCs was also readily spin-cast on polyimide ($T_g$ ~360 °C). Our synthesis and assembly provide a promising solution to the fabrication of transparent and conducting ITO NCs on flexible substrates for optoelectronic applications.

## EXPERIMENTAL SECTION

**Synthesis of 11 nm ITO NCs with Sn at 10 atom %.** A mixture of indium acetylacetonate ($In(acac)_3$) (300 mg, 0.73 mmol), tin bis(acetylacetonate)dichloride, ($Sn(acac)_2Cl_2$) (30 mg, 0.078 mmol), oleylamine (3 mL), and 1-octadecene (17 mL) was stirred under $N_2$ flow in a four-neck flask with a distillation setup. This mixture was heated to 250 °C for 30 min at 10 °C/min. After 30 min, oleic acid (1 mL) was added, and the mixture was heated to 270 °C for an additional hour. After it was cooled to room temperature, 30 mL of isopropyl alcohol was added. The product was separated by centrifugation, and the precipitated NCs were redispersed in 20 mL of hexane in the presence of oleylamine (0.2 mL) and oleic acid (0.2 mL). Twenty milliliters of ethanol was added to flocculate the NCs, which were then separated by centrifugation. The process was repeated once, and the final product, ITO NCs, was dispersed in hexane for further use. In the synthesis, the amount of Sn precursor added was used to control Sn composition in ITO NCs.

**Preparation of ITO NC Assembly.** An 18 × 18 $mm^2$ large glass substrate was first dried in an oven at 140 °C overnight. A total of 0.2 mL of the ITO NC dispersion in hexane was spin-cast onto the glass substrate at 5000 rpm for 35 s. To control the assembly thickness, concentrations of the ITO NC dispersion were controlled from 13 to 90 mg/mL, which resulted in 23−146 nm thick NC assemblies. The backside of the substrate was wiped clean with a hexane-soaked Kimwipe. Finally, the ITO-coated substrate was annealed under a gas mixture of Ar and 5% $H_2$ at 300 °C for the designated time.

**Characterization of ITO NC and Their Assemblies.** One drop of the as-synthesized ITO NC dispersion (~0.5 mg/mL) was placed onto carbon-coated copper grids, and hexane was allowed to evaporate at room temperature. TEM and HRTEM images were taken on a Phillips EM-420 TEM and a JEOL JEM-2010 TEM, respectively. X-ray diffraction (XRD) patterns were collected on a Bruker D8 Advance X-ray diffractometer with Cu K$\alpha$ radiation ($\lambda$ = 1.5418 Å). Surface and cross-sectional SEM images of the ITO NC assemblies were obtained on a LEO 1530. Composition of ITO NCs was analyzed by ICP-AES. To study the growth process of ITO NCs, an aliquot of the reaction solution was withdrawn at different times. The thickness of the NC assemblies was measured by ellipsometry. Using the ellipsometric data, the packing density of the NC assemblies was determined by Maxwell-Garnett effective medium approximation (EMA) (Supporting Information).[21] For ellipsometry measurements, ITO NCs were spin-cast onto Si substrates under the same conditions mentioned above because of the difficulty in measuring the thickness of ITO assemblies on glass substrates. Sheet resistance of the ITO NC assemblies was obtained by four-point probe measurements and the van der Pauw method over the 18 × 18 $mm^2$ glass substrate. The Hall Effect was measured by the van der Pauw method. Regional roughness was analyzed by a Veeco D3100 AFM. Transmittance of the ITO NC assemblies on glass substrates was measured by a PerkinElmer Lambda 35 UV−vis absorption spectrophotometer in the wavelength range between 300 and 1100 nm.

## RESULTS AND DISCUSSION

Monodisperse ITO NCs were synthesized by the thermal decomposition of $In(acac)_3$ and $Sn(acac)_2Cl_2$ at 270 °C in 1-octadecene with oleylamine and oleic acid as surfactants for NC growth and passivation. These two metal precursors were specifically chosen to prepare ITO NCs because they decompose at a similar temperature, which facilitates the doping of $Sn^{4+}$ into $In_2O_3$. Different metal precursors, such as metal acetates and metal chlorides, were also tested but failed to yield good quality ITO NCs. Figure 1a shows the transmission electron microscopy (TEM) image of typical monodisperse ITO NCs prepared using this synthetic approach. The NCs have an average diameter of 11.0 ± 0.6 nm and are prone to self-assemble into a NC superlattice. Dynamic light scattering (DLS) measurements confirm that the hydrophobic ITO NCs are stable for months in a nonpolar or weakly polar solvent such as hexane, toluene, or chloroform, as their hydrodynamic size in a hexane dispersion showed no measurable change over a four-month period (Figure S1). The XRD pattern of these


dx.doi.org/10.1021/ja3044807 | J. Am. Chem. Soc. 2012, 134, 13410−13414

NC assemblies (Figure 1b) indicates that the NCs have the basic $In_2O_3$ cubic bixbyite structure. The average grain size estimated from the (222) peak broadening and Scherrer's equation is 8.1 nm, which is close to the size measured by TEM. The NC structure is further analyzed by high-resolution TEM (HRTEM) (Figure 1c), from which we observe that the representative NC is a single crystal with a lattice fringe distance of 0.91 nm, illustrative of the crystal lattice spacing of the (222) planes.

The Sn composition in ITO NCs was tuned by the amount of $Sn(acac)_2Cl_2$ used in the reaction mixture. For example, 0.07 mmol of $Sn(acac)_2Cl_2$ and 0.7 mmol of $In(acac)_3$ yielded ITO NCs containing 10% Sn. However, when the Sn amount exceeded 15%, the NC shape could no longer be controlled (Figure S2), which is likely the result of the distortion in the $In_2O_3$ crystal structure caused by the high percentage substitution of $In^{3+}$ by $Sn^{4+}$. With increasing Sn%, the final color of ITO NCs varies from yellow to blue (Figure 1d), as $Sn^{4+}$ dopants provide electrons to the conduction band of ITO, and these free electrons are responsible for the surface plasmon resonance in the near-infrared region that gives the dispersion its blue color.[3,16] During the synthesis of ITO with Sn 10%, the color of the reaction solution gradually changed from yellow to green and finally to blue. TEM analysis indicated that the ITO NCs began to form when the temperature reached 250 °C, and ICP-AES revealed that the Sn composition in ITO NCs was maintained throughout the synthesis (Figure S3 and Table S1).

The monodisperse ITO NCs were assembled on a glass substrate by spin-coating the ITO NC dispersion in hexane. The thickness of the assemblies was controlled by varying the concentrations of ITO NC dispersions cast on the glass surface. When 0.2 mL of 13, 30, 50, 65, and 90 mg/mL concentrations of ITO dispersions were spin-cast onto a 3.24 $cm^2$ large square substrate, assemblies that were 28, 63, 90, 123, and 146 nm thick, respectively, were produced. To ensure the close packing of NCs, the assemblies were annealed at 300 °C under Ar and 5% $H_2$ for 6 h. All assemblies appeared uniform over a 20 $\mu m^2$ area, as seen from the scanning electron microscopy (SEM) images (Figure 2a,b). Analysis of atomic force microscopy (AFM) images of the assemblies indicates that these assemblies have a very smooth surface over a 25 $\mu m^2$ area with a root-mean-square surface roughness of 2.9 nm (Figure S4). The cross-sectional SEM image of the 80 nm thick assembly (Figure 2c) shows that the ITO NCs stack densely with no visible cracks or pores. The packing density of the NC assemblies determined by the Maxwell-Garnett EMA is greater than 70% over the entire thickness range (Figure S5).

To achieve efficient charge transport within the ITO NC assemblies, we annealed these assemblies at different conditions and measured their resistivities. When the 120 nm thick ITO NC assemblies (Sn ~10%) were annealed at 300 °C for 6 h under Ar and 5% $H_2$; Ar; and air, their resistivity values were $6.8 \times 10^{-3}$, $1.3 \times 10^{-1}$, and $7.4 \times 10^{-1}$ Ω·cm, respectively. The low resistivity from the assembly annealed under Ar and 5% $H_2$ is a result of an increase in both oxygen vacancies and electrically activated $Sn^{4+}$ doping in ITO NCs.[22] The effect of surfactant on assembly resistivity was also studied on the assemblies annealed under Ar and 5% $H_2$ at 300 °C. The 120 nm thick assemblies annealed for 3 and 6 h exhibited resistivity values of $1.2 \times 10^{-2}$ and $6.8 \times 10^{-3}$ Ω·cm, respectively. Longer annealing times (over 6 h) did not lead to significant resistivity improvements. Infrared (IR) spectra of the 6 h annealed ITO assembly show no obvious C−H stretches from the surfactants

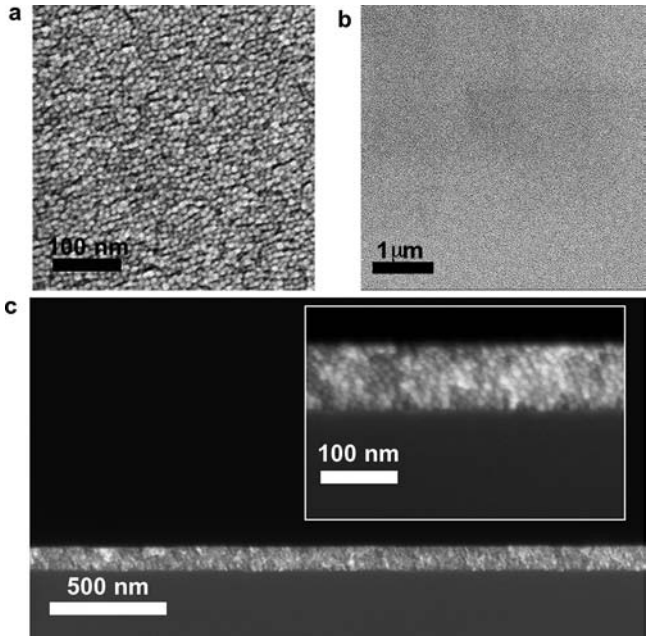


**Figure 2.** ITO NC assemblies fabricated from the spin-casting method on glass substrates. (a and b) SEM images of the ITO NC assembly at different magnifications; (c) SEM image of a cross-sectional view of an 80 nm thick ITO NC assembly. Inset: higher resolution SEM image of the cross-sectional view of the 80 nm ITO NC assembly. The assemblies were annealed at 300 °C under Ar and 5% $H_2$ for 6 h.

(Figure S6), indicating the absence of the original surfactants in the ITO NC assembly annealed for 6 h. Detailed SEM analyses on the annealed assemblies show no evidence for NC aggregation/sintering or cracks within the assemblies.

Sn composition exhibits a strong effect on the resistivity of the ITO NC assemblies. Figure 3a shows the Sn-composition-dependent resistivities of the 120 nm ITO NC assemblies annealed under Ar and 5% $H_2$ at 300 °C for 6 h. We see that when $Sn^{4+}$ is doped into $In_2O_3$ in small percentages (ca. 0−5%), the resistivity value of the assemblies decreases sharply with increasing $Sn^{4+}$ doping level, but beyond 10%, the resistivity increases. This resistivity trend is consistent with previous studies of Sn doping on the resistivity of ITO thin films. At low Sn %, most $Sn^{4+}$ doping provides free electrons, increasing the carrier density; beyond 4% Sn concentrations, a larger fraction of Sn doping becomes electrically inactive.[22,23] As a result, the carrier density is maximized at Sn ~10%.[22,24,25] On the contrary, the mobility decreases with increasing Sn % due to enhanced ionized impurity scattering and phonon scattering.[22,24,25] Combined changes in the carrier density and the mobility result in the lowest resistivity in Sn concentrations of 5−10%.[22,24,25] The ITO assemblies also show thickness-dependent resistivities (Figure 3b). For assemblies with Sn composition fixed at 10%, the resistivity decreases rapidly up to thickness values of 95 nm and then remains relatively constant. For an ITO NC film that is 146 nm thick with 10% Sn doping, the resistivity reaches $5.2 \times 10^{-3}$ Ω·cm ($R_s$ = 356 Ω/sq)—the lowest value ever reported for NC-based ITO thin-film assemblies.

To understand the charge transport mechanism in ITO NC assemblies, we measured the Hall Effect of the assemblies. The changes of assembly mobility and carrier density with assembly thickness are shown in Figure 3b. We find that with increasing assembly thickness, the carrier densities increase while the


dx.doi.org/10.1021/ja3044807 | J. Am. Chem. Soc. 2012, 134, 13410−13414

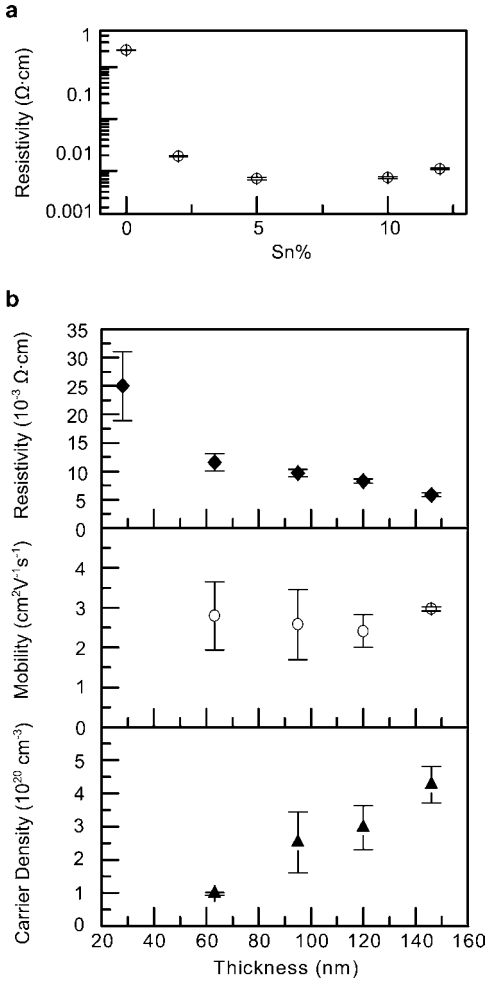


**Figure 3.** (a) Resistivity changes in 120 nm ITO NC assemblies as a function of the Sn atomic percentage; the *y*-axis is in logarithm scale. (b) Resistivity, mobility and carrier density changes as a function of the thickness of the ITO NC assemblies with ITO NCs containing 10% Sn. The assemblies were annealed at 300 °C under Ar and 5% $H_2$ for 6 h. The error bars were from the measurements of five different samples.

mobility values are relatively stable. Figure S5 shows that the packing density of the ITO NC assemblies increases from 75 to 84% in the thickness range 63−146 nm. As higher packing density (or less porosity) leads to a larger number of charge carriers in a given volume, the increase in the carrier density here should be the result of the increase in packing density in thicker assemblies. Note that we did not report the carrier density of the 28 nm thick assembly because the carrier density was too small to generate a Hall voltage that could be measured by our Hall measurement system. In addition, the effect of thermal annealing on charge transport in the 146 nm thick ITO NC assemblies was studied and compared with the sputtered ITO film (Table 1). We found that the carrier densities in the ITO NC assemblies studied were nearly identical, but the Hall mobilities increased with longer annealing times and higher annealing temperatures. Compared with Assembly 1, Assembly 2 has nearly double the Hall mobility, indicating that annealing for a longer time facilitates the removal of surfactants and enhances charge transport within the assembly. The surfactant removal is further confirmed by IR analysis of the annealed assemblies (Figure S6). The assembly annealed at 400 °C (Assembly 3) exhibits a smaller resistivity at $1.8 \times 10^{-3}$ Ω·cm, predominantly because of the large mobility present in the assembly structure. However, this annealing condition resulted in partial aggregation of ITO NCs and shrinkage in the assembly (Figure S7) that also partially destroyed transparency of the assembly. Compared with the data from the sputtered ITO thin film (Table 1), the low mobility observed from the current ITO NC assemblies is likely caused by the charge scattering from the smaller ITO grain sizes and defects in the NC assemblies.

The highly conductive ITO NC assemblies are also transparent in the visible spectral range. Figure 4 shows the

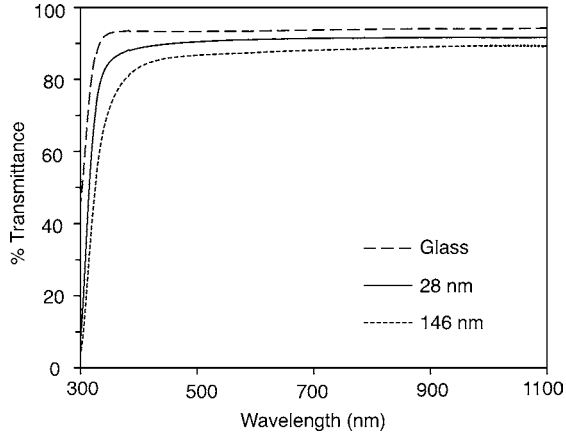


**Figure 4.** Percent transmittance of the glass substrate, the 28 nm thick ITO NC assembly on the glass substrate, and the 146 nm thick ITO NC assembly on the glass substrate measured in the wavelength range from 300 to 1100 nm.

UV−vis spectra of the glass substrate and ITO NC assemblies annealed at 300 °C for 6 h under Ar + 5% $H_2$. The transparency of ITO NC assemblies is reduced slightly by the glass substrate, with the thinner assembly having a slightly higher optical transmittance. The highly conductive 146 nm thick assembly has transparency greater than 85% in the visible spectral range when the glass substrate background is included. With the exclusion of the glass substrate effect, the assembly has

**Table 1. Electrical Properties of ITO NC Assemblies Annealed under Different Conditions**

| | annealing condition | thickness (nm) | resistivity ($10^{-3}$ Ω·cm) | sheet resistance (Ω/sq) | carrier density ($10^{20}$ $cm^{-3}$) | hall mobility ($cm^2V^{-1}s^{-1}$) | grain size[a] (nm) |
|---|---|---|---|---|---|---|---|
| Assembly 1 | 300 °C 3 h | 146 | 14 | 935 | 2.7 | 1.7 | 13 |
| Assembly 2 | 300 °C 6 h | 146 | 5.2 | 358 | 4.1 | 2.9 | 13 |
| Assembly 3 | 400 °C 6 h | 146 | 1.8 | 118 | 2.8 | 12.5 | 11 |
| Sputtered ITO[b] | Sputtered at 400 °C | 137 | 0.13 | 9 | 10.5 | 42.9 | 22 |

[a]Grain size was estimated from Scherrer's equation based on the analysis of the (222) peak broadening in the related XRD pattern. [b]Data from ref 4.


dx.doi.org/10.1021/ja3044807 | J. Am. Chem. Soc. 2012, 134, 13410−13414

a transparency of 93%. The high transparency and low resistivity ($5.2 \times 10^{-3}$ Ω·cm) exhibited by the 146 nm thick ITO NC assembly already meet the requirements for electrodes used in resistive touch panels.[26]

The high performance in both electrical conductivity and optical transparency of the ITO NC assembly can be attributed to the monodispersity of the ITO NCs prepared from our unique solution-phase synthesis and the high degree of uniformity in the thin-film assembly achieved via spin-casting. A stable dispersion of monodisperse NCs is the most important factor for an assembly to achieve a densely packed structure. Any degree of aggregation of ITO NCs in the dispersion would deteriorate the uniformity of the assembly produced from the same spin-casting process, as demonstrated by the rough surface shown in one assembly prepared from a dispersion of partially aggregated NCs (Figure S8). Consequently, such a low quality ITO NC assembly has a resistivity value of $1.6 \times 10^{-1}$ Ω·cm, even after annealing under Ar and 5% $H_2$ at 300 °C for 6 h, which is the optimum condition we apply to treat all of our ITO NC assemblies. Furthermore, the long hydrocarbon chains present in the oleic acid and oleylamine surfactants, ca. 2.5 nm long, are also responsible for the higher resistivity values in the as-prepared ITO NC assemblies. Controlled thermal annealing under Ar and 5% $H_2$ at 300 °C for 6 h is necessary to achieve low resistivity in the assembly without causing NC aggregation/sintering. We also tested the spin-casting process on a polymer substrate (polyimide, $T_g$ ~360 °C) and found that the assembly and annealing process worked equally well on this polymer substrate—the 120 nm ITO NC assembly exhibited a resistivity of $7 \times 10^{-3}$ Ω·cm. As a comparison, an ITO film deposited on a polymer substrate via sputtering at room temperature has a resistivity of ca. $7 \times 10^{-4}$ Ω·cm.[27]

## CONCLUSION

We have presented a facile synthesis of monodisperse ITO NCs with controlled size (11 nm) and Sn composition (0−12%). The monodisperse ITO NCs are assembled uniformly via a spin-casting process on a centimeter-wide glass substrate with a root-mean-square roughness of 2.9 nm. Controlled annealing is applied to treat the assemblies, and their conductivities are dependent both on the Sn concentration and the assembly thickness. The 146 nm thick ITO assembly annealed under Ar and 5% $H_2$ at 300 °C for 6 h exhibits the lowest resistivity at $5.2 \times 10^{-3}$ Ω·cm and greater than 93% transparency in the visible spectral range, achieving the best performance reported to date for an ITO NC assembly. This excellent performance is attributed to NC monodispersity and stability in solution, which are critical characteristics for making uniform and densely packed NC assemblies on a solid support. Furthermore, our synthesis and assembly process is not limited to glass substrates but can be extended to polymer films as well. With proper surface coating control, these monodisperse and stable ITO NCs should function as unique building blocks for fabricating ITO NC assemblies on flexible surfaces with high electrical conductivity and optical transparency for future optoelectronic applications.

## ASSOCIATED CONTENT

### Supporting Information

DLS, TEM, ICP-AES, AFM, IR, SEM images and description for determining packing density of the ITO NC assemblies. This material is available free of charge via the Internet at http://pubs.acs.org.

## AUTHOR INFORMATION


### Corresponding Author

ssun@brown.edu


### Notes

The authors declare no competing financial interest.

## ACKNOWLEDGMENTS

The work was supported by Advanced Technology Materials, Inc. (ATMI).

## REFERENCES


(1) Kim, H.; Gilmore, C. M.; Piqué, A.; Horwitz, J. S.; Mattoussi, H.; Murata, H.; Kafafi, Z. H.; Chrisey, D. B. *J. Appl. Phys.* **1999**, *86*, 6451.
(2) Martinez, M. A.; Herrero, J.; Gutierrez, M. T. *Thin Solid Films* **1995**, *269*, 80.
(3) Tahar, R. B. H.; Ban, T.; Ohya, Y.; Takahashi, Y. *J. Appl. Phys.* **1998**, *83*, 2631.
(4) Shigesato, Y.; Takaki, S.; Haranoh, T. *J. Appl. Phys.* **1992**, *71*, 3356.
(5) Cairns, D. R.; Witte, R. P.; Sparacin, D. K.; Sachsman, S. M.; Paine, D. C.; Crawford, G. P.; Newton, R. R. *Appl. Phys. Lett.* **2000**, *76*, 1425.
(6) Dattoli, E. N.; Lu, W. *MRS Bull.* **2011**, *36*, 782.
(7) Hong, H.; Jung, H.; Hong, S.-J. *Res. Chem. Intermed.* **2010**, *36*, 761.
(8) Jeong, J.-A.; Lee, J.; Kim, H.; Kim, H.-K.; Na, S.-I. *Sol. Energy Mater. Sol. Cells* **2010**, *94*, 1840.
(9) Buhler, G.; Tholmann, D.; Feldmann, C. *Adv. Mater.* **2007**, *19*, 2224.
(10) Sun, S.; Murray, C. B.; Weller, D.; Folks, L.; Moser, A. *Science* **2000**, *287*, 1989.
(11) Urban, J. J.; Talapin, D. V.; Shevchenko, E. V.; Murray, C. B. *J. Am. Chem. Soc.* **2006**, *128*, 3248.
(12) Coe-Sullivan, S.; Steckel, J. S.; Woo, W.-K.; Bawendi, M. G.; Bulovic, V. *Adv. Funct. Mater.* **2005**, *15*, 1117.
(13) Furube, A; Yoshinaga, T.; Kanehara, M.; Eguchi, M.; Teranishi, T. *Angew. Chem., Int. Ed.* **2012**, *51*, 2640.
(14) Ederth, J.; Heszler, P.; Hultaker, A.; Niklasson, G. A.; Granqvist, C. G. *Thin Solid Films* **2003**, *445*, 199.
(15) Fang, J. Y.; Sun, Z. Y.; He, J. B.; Kumbhar, A. *Langmuir* **2010**, *26*, 4246.
(16) Wang, T.; Radovanovic, P. V. *J. Phys. Chem. C* **2011**, *115*, 406.
(17) Kanehara, M.; Koike, H.; Yoshinaga, T.; Teranishi, T. *J. Am. Chem. Soc.* **2009**, *131*, 17736.
(18) Sasaki, T; Endo, Y.; Nakaya, M.; Kanie, K.; Nagatomi, A.; Tanoue, K.; Nakamura, R.; Muramatsu., A. *J. Mater. Chem.* **2010**, *20*, 8153.
(19) Ba, J.; Rohlfing, D. F.; Feldhoff, A.; Brezesinski, T.; Djerdj, I.; Wark, M.; Niederberger, M. *Chem. Mater.* **2006**, *18*, 2848.
(20) Choi, S. Y.; Kim, S. S.; Park, C. G.; Jin, H. W. *Thin Solid Films* **1999**, *347*, 155.
(21) Himcinschi, C.; Friedrich, M.; Murray, C.; Streiter, I.; Schulz, S. E.; Gessner, T.; Zahn, D. R. T. *Semicond. Sci. Technol.* **2001**, *16*, 806.
(22) Frank, G.; Köstlin, H. *Appl. Phys. A: Mater. Sci. Process.* **1982**, *27*, 197.
(23) Shigesato, Y.; Paine, D. C. *Appl. Phys. Lett.* **1993**, *62*, 1268.
(24) Mizuhashi, M. *Thin Solid Films* **1980**, *70*, 91.
(25) Sato, Y.; Tokumaru, R.; Nishimura, E.; Song, P. −K.; Shigesato, Y.; Utsumi, K.; Iigusa, H. *J. Vac. Sci. Technol., A* **2005**, *23*, 1167.
(26) Hecht, D. S.; Hu, L.; Irvin, G. *Adv. Mater.* **2011**, *23*, 1482.
(27) Kim, H.; Horwitz, J. S.; Kushto, G. P.; Kafafi, Z. H.; Chrisey, D. B. *Appl. Phys. Lett.* **2001**, *79*, 284.